BNL-224590-2023-JAAM

Investigation of Electron Extraction and Protection Layers on Cu2O Photocathodes

D. Wi, M. Liu

To be published in "Chemistry of Materials"

May 2023

Center for Functional Nanomaterials

Brookhaven National Laboratory

U.S. Department of Energy

USDOE Office of Science (SC), Basic Energy Sciences (BES) (SC-22)

DISCLAIMER

Investigation of Electron Extraction and Protection Layers on Cu_2O Photocathodes

Dae Han Wi,[1] Margaret A. Lumley,[1] Zhaoyi Xi,[2,3] Mingzhao Liu,[2] and Kyoung-Shin Choi[1,*]

[1]*Department of Chemistry, University of Wisconsin-Madison, Madison, WI 53706, United States.*
[2]*Center for Functional Nanomaterials, Brookhaven National Laboratory, Upton, NY 11973, United States*
[3]*Department of Materials Science and Chemical Engineering, Stony Brook University, Stony Brook, NY 11794, United States*

* Correspondence and requests for materials should be addressed to K.-S.C. (email: kschoi@chem.wisc.edu).

Abstract

Many semiconductor photoelectrodes used for solar fuel production require the addition of buffer and protection layers to enhance their solar-to-fuel conversion efficiency and long-term stability. For example, Cu_2O, which is the most efficient oxide-based photocathode but suffers from photocorrosion, has been assembled with various buffer and protection layers to suppress photocorrosion and use more photoexcited electrons for useful reactions such as water reduction to H_2. However, the abilities of various buffer and protection layers to extract electrons from Cu_2O have never been directly evaluated. Instead, their abilities were estimated based on the photocurrent for water reduction after adding a hydrogen evolution catalyst on top of them. In these evaluations, as the photocurrent is affected not only by the buffer or protection layer but also by the catalyst, the ability of the buffer or protection layer to extract electrons from Cu_2O could not be accurately determined or compared. In this study, we demonstrate that 4-hydroxy-2,2,6,6-tetramethylpiperidine-1-oxyl (TEMPOL), whose reduction rate is faster than the photocorrosion rate of Cu_2O, can be used as an effective electron scavenger to directly evaluate any change caused by a buffer or protection layer in electron-hole separation in Cu_2O. In particular, we compared the performances of ZnO and TiO_2 layers on Cu_2O for extracting electrons and suppressing photocorrosion. We also compared the performances of TiO_2 layers prepared by electrodeposition and atomic layer deposition (ALD) to show that the deposition method can make a striking impact on the performance of the same TiO_2 because it can affect the critical characteristics of the layer (e.g., defect levels, conductivity, interfacial atomic arrangements) that govern interfacial charge transfer in multilayer photoelectrodes.

Introduction

Cu_2O is an inexpensive, narrow-bandgap (~2.1 eV) p-type oxide that has been investigated as a photocathode in a photoelectrochemical cell for water reduction to H_2, CO_2 reduction, and N_2 reduction to NH_3.[1-3] In particular, Cu_2O has been reported to generate the highest photocurrent for solar hydrogen production among all oxide-based photocathodes.[4-8] However, Cu_2O photocathodes suffer from photocorrosion (i.e., cathodic photocorrosion of Cu_2O to Cu by photoexcited electrons) that is thermodynamically and kinetically very favorable.[1] Fortunately, recent studies have demonstrated that the photostability of Cu_2O can be significantly enhanced by adding a TiO_2 protection layer that is chemically and electrochemically stable under a wide range of reaction conditions.[1,5-9] Studies of Cu_2O photocathodes using TiO_2 as a protection layer commonly reported that a buffer layer (e.g., ZnO, Ga_2O_3) is necessary between the Cu_2O and TiO_2 layers.[1,5-8] Without the buffer layer, the photocurrent generated by Cu_2O/TiO_2/Pt, where Pt served as a hydrogen evolution catalyst, was lower than that generated by Cu_2O/Pt, suggesting a considerable recombination loss at the Cu_2O/TiO_2 interface.[1] Furthermore, no improvement in photostability was observed without the buffer layer.[1]

A material that can be used as a protection layer to suppress photocorrosion should be chemically and electrochemically inert and also be able to rapidly extract surface-reaching minority carriers (i.e., electrons for p-type Cu_2O) from the underlying photoelectrode before they are accumulated and used for undesired surface recombination or photocorrosion of the photoelectrode. The chemical and electrochemical inertness of TiO_2 makes it an ideal candidate to serve as a protection layer for Cu_2O and other photoelectrodes.[10-14] As the conduction band minimum (CBM) of TiO_2 is lower than that of Cu_2O,[1] it should also have no thermodynamic issue in extracting photoexcited electrons from the conduction band (CB) of Cu_2O. Thus, in principle, TiO_2 should not need an additional electron extraction layer (i.e., buffer layer) between Cu_2O and TiO_2. This raises a question as to whether the reported requirement for an additional buffer layer is due to intrinsic features of TiO_2 or due to specific features of TiO_2 prepared by atomic layer deposition (ALD) that was commonly used in previous studies.[1,5-8]

To date, the ability of the TiO_2 layer or other buffer layers to extract electrons from the Cu_2O layer has been evaluated by measuring the photocurrent for the hydrogen evolution reaction (HER).[1,5-8] However, since TiO_2 or other materials used as buffer layers are not catalytic for HER, the photocurrent for HER was obtained after an HER catalyst was added to these layers. In this

case, because the photocurrent for HER is affected not only by the buffer or protection layer but also by the HER catalyst (e.g., even the same HER catalyst can be deposited differently on different buffer and protection layers), the observed difference in photocurrent for HER cannot be solely and directly related to the difference in the ability of the buffer and protection layers to extract electrons from Cu_2O.

The most direct and straightforward way to examine the ability of buffer and protection layers to extract electrons from Cu_2O is to measure photocurrent using an electron scavenger that has fast reduction kinetics. Then, if the presence of a buffer or protection layer helps suppress photocorrosion or electron-hole recombination in Cu_2O, thus increasing the number of surface-reaching electrons available for interfacial reduction reactions, it will directly result in an increase in photocurrent for the reduction of the electron scavenger. This means that any change in photocurrent obtained with the electron scavenger can be directly linked to the effect of the buffer or protection layer in altering the number of electrons extracted from Cu_2O. Unfortunately, the rate of cathodic photocorrosion in Cu_2O is extremely fast and finding an electron scavenger with a reduction rate faster than its photocorrosion rate has been challenging. If the reduction rate of an electron scavenger is slower than the photocorrosion rate, the measured photocurrent is primarily due to photocorrosion and not due to the reduction of the electron scavenger. In this case, the photocurrent density cannot be accurately related to the number of surface-reaching electrons available for desired interfacial chare transfer reactions because photocorrosion increases the number of recombination sites, directly and progressively affecting the degree of electron-hole recombination.

In this study, we report an electron scavenger whose reduction rate is sufficiently fast to kinetically suppress photocorrosion in Cu_2O. Using this electron scavenger, we were able to straightforwardly examine the ability of ZnO and TiO_2 layers to extract electrons from Cu_2O without needing to deposit HER catalysts on ZnO and TiO_2. We also compared the performances of electrodeposited and ALD-deposited TiO_2 layers on Cu_2O to probe whether the previous finding that TiO_2 cannot serve as an efficient electron extraction layer for Cu_2O is due to intrinsic issues of the Cu_2O/TiO_2 junction regardless of the deposition method or whether it is only for the ALD-deposited TiO_2 layer. This study offers an effective method to investigate and compare the performance of electron extraction layers on a Cu_2O photocathode as well as new insights into the factors that affect their performances.

Experimental

Chemicals and Materials. Copper(II) sulfate pentahydrate ($CuSO_4 \cdot 5H_2O$, ≥98.0%), DL-lactic acid ($CH_3CH(OH)COOH$, 85%), potassium hydroxide (KOH, ≥85%), 4-hydroxy-TEMPO ($C_9H_{18}NO_2$, 97%), and *p*-benzoquinone ($C_6H_4O_2$, ≥98.0%) were purchased from Sigma-Aldrich. Zinc nitrate hexahydrate ($Zn(NO_3)_2 \cdot 6H_2O$, ≥98%) was purchased from Strem Chemicals. Boric acid (H_3BO_3, 99.8%) and ammonium bis(oxalate)oxotitanate(IV) hydrate ($(NH_4)_2TiO(C_2O_4)_2 \cdot xH_2O$ (x≈1), 99.998%) were purchase from Alfa Aesar. Potassium phosphate monobasic (KH_2PO_4, >99.96%) was purchased from Electron Microscopy Sciences. Dimethyl sulfoxide ($(CH_3)_2SO$, ≥99.9%) was purchased from VWR International. All aqueous solutions of the chemicals were prepared with highly purified deionized water (resistivity > 18.0 MΩ).

Preparation of Cu_2O electrodes. Cu_2O electrodes were prepared using a previous reported electrodeposition method.[3,15] Au-coated and Pt-coated glasses (LGA Thin Films) that were prepared by sputter deposition of Au or Pt on the top of Ti (20 nm)-deposited glass slides were used as the working and counter electrode respectively. A double-junction Ag/AgCl electrode (4 M KCl) was used as the reference electrode. A multichannel potentiostat (Biologic VMP2) was used for the electrodeposition. An aqueous solution containing $CuSO_4 \cdot 5H_2O$ (20 mM), KH_2PO_4 (50 mM) and DL-lactic acid (0.4 M) was used as a plating solution after adjusting the pH to 12 with KOH. The cathodic electrodeposition was performed at a constant potential of –0.46 V vs. Ag/AgCl (0.45 V vs. RHE) at 60 °C for 14 min 30 s (~1 C/cm^2). After deposition, the resulting films were rinsed with water and dried with a stream of air.

Electrodeposition of ZnO on Cu_2O electrodes. For the electrodeposition of ZnO on Cu_2O, the prepared Cu_2O film was used as the working electrode and Pt-coated glass was used as the counter electrode. A double-junction Ag/AgCl electrode (4 M KCl) was used as the reference electrode. To prepare a plating solution, $Zn(NO_3)_2 \cdot 6H_2O$ (50 mM) and *p*-benzoquinone (*p*-BQ) (100 mM) were dissolved in dimethyl sulfoxide (DMSO) (20 mL). After heating the solution to 95 °C, 0.5 mL of water was added, and the cathodic electrodeposition of ZnO was carried out galvanostatically at a constant current density of –0.11 mA/cm^2 for 7 min 35 s (~50 mC/cm^2). During electrodeposition, *p*-BQ is reduced to hydroquinone (HQ) (*p*-BQ + $2H^+$ + $2e^-$ ⇌ HQ),

elevating the local pH on the WE and lowering the solubility of Zn^{2+}.[16] As a result, Zn^{2+} is precipitated as ZnO on the Cu_2O electrode. This electrodeposition method is based on the method published in our previous paper[17] with a modification that *p*-BQ reduction instead of nitrate reduction is used to increase the pH. ZnO films electrodeposited from a DMSO solution at ≥ 85 °C were reported to be highly transparent and crystalline.[17] After the deposition, the resulting films were rinsed with water and dried with a stream of air.

Electrodeposition of TiO_2 layer on Cu_2O electrodes. For the electrodeposition of TiO_2 on Cu_2O, a DMSO solution containing $(NH_4)_2TiO(C_2O_4)_2 \cdot xH_2O$ (x≈1) (2 mM) and *p*-BQ benzoquinone (100 mM) was used as the plating solution. After heating the solution (20 mL) to 95 °C, the cathodic electrodeposition was carried out at a constant potential of –0.1 V for 2 min (~10 mC/cm^2). This electrodeposition method of TiO_2 is based on the method published in our previous paper,[11] but we used a DMSO solution instead of an aqueous solution in this study. The deposition mechanism used here is the same as that used for ZnO deposition (i.e., electrochemical increase of the pH by *p*-BQ reduction). We found that water contained in the Ti precursor and dimethyl sulfoxide was sufficient to deposit a thin TiO_2 layer (~ 5 nm) and no additional water was added to the plating solution. (Adding water results in the deposition of thicker TiO_2. layers.) After the deposition, the resulting films were rinsed with ethanol and dried with a stream of air. Then, the as-deposited film was annealed in a tube furnace at 200 °C for 2 h with N_2 flow (ramping rate: 3 °C/min). After annealing, the furnace was cooled down to room temperature. After the deposition, the surface of Cu_2O underneath the TiO_2 layer was analyzed by Cu LMM X-ray photoelectron spectroscopy (XPS) to confirm that Cu^0 was not formed during the electrodeposition of the TiO_2 layer (**Figure S1**). The ZnO layer in Cu_2O/ZnO was too thick (~100 nm) to perform the same XPS analysis of the underlying Cu_2O surface. However, we note that the potential used for the electrodeposition of ZnO was more positive than that used for the electrodeposition of TiO_2. Thus, we can rationally assume that no Cu^0 was formed during the electrodeposition of ZnO.

Atomic layer deposition of TiO_2 on Cu_2O. A TiO_2 layer was deposited on Cu_2O using an atomic layer deposition (ALD) system (Cambridge Nanotech Savannah S100), at a substrate temperature of 120˚C, using vapors of titanium isopropoxide (preheated to 80˚C) and water as precursors. The deposition was carried out under 590 mTorr of nitrogen carrier gas flowing at 20 sccm and had a nominal deposition rate 0.0407 nm/cycle. The nominal deposition rate was determined by

depositing TiO_2 on silicon wafers using various cycle numbers (50-300) and determining the resulting TiO_2 layer thicknesses by spectroscopic ellipsometry (J.A. Woollam, M-2000). A linear fitting between ALD cycle numbers and TiO_2 thicknesses gave the nominal deposition rate. Given that both silicon and Cu_2O have hydrophilic surfaces, it is assumed that the deposition rate of TiO_2 on these two substrates are comparable. For a thickness of 5 nm, a total of 123 ALD cycles was conducted.

Characterization. The surface morphologies of the films were investigated by a scanning electron microscope (Zeiss Supra VP55) with an operating voltage of 3 eV. The crystallographic structures of the samples were investigated with an X-ray diffractometer (Bruker D8 Discover) with a Cu Kα (λ = 1.54178 Å) radiation source. The oxidation states of metal ions in Cu_2O and TiO_2 were analyzed with an X-ray photoelectron spectrometer (Thermo K alpha X-ray Photoelectron Spectrometer) with Al K*a* X-ray source. For the calibration of XPS data, the C 1s peak at 284.8 eV was used as reference. Transmission electron microscopy (TEM) images of Cu_2O/TiO_2 samples were collected with a field emission transmission electron microscope (FEI Tecnai TF 30) operated at 300 kV.

Photoelectrochemical Characterization. All photoelectrochemical measurements were conducted in an undivided quartz cell with a three-electrode set-up using an SP-200 potentiostat/EIS (Bio-Logic Science Instrument). The photoelectrode was masked with lacquer to expose an identical geometric area (0.02 cm^2) smaller than the illuminated area (0.06 cm^2). A Pt electrode described above was used as the counter electrode and a single-junction Ag/AgCl electrode (4 M KCl) was used as the reference electrode. Potentials measured against the Ag/AgCl electrode were converted to potentials against the reversible hydrogen electrode (RHE) using the following equation:

$$E\ (\text{vs. RHE}) = E\ (\text{vs. Ag/AgCl}) + 0.1976 + 0.0591 \times \text{pH}$$

Solar illumination was simulated by filtering light from a 300 W Xe arc lamp (a Newport 66902 power supply with Ushio Xenon short arc lamp) through the following successive filters: water IR filter, neutral density filters, and an AM 1.5 G filter. The light was collimated and directed onto the sample via an optical fiber, and the light was calibrated to 100 mW/cm^2 (1 sun) using an NREL-certified GaAs reference cell (PV Measurements).

A 0.25 M borate buffer solution (pH 10.6) with and without TEMPOL (100 mM) was used as the electrolyte for water reduction and TEMPOL reduction, respectively. We originally chose this pH condition to examine the electron extraction ability of the ZnO layer without being concerned about its chemical dissolution. (ZnO is amphiphilic and is the least soluble around pH 10.6) but later found that this condition is also optimal in achieving the highest photocurrent for TEMPOL reduction. Before the photocurrent measurement, the electrolyte was purged with Ar for 30 minutes to degas dissolved O_2. The electrolyte was continuously purged with Ar and gently stirred with a magnetic stirring bar during the photoelectrochemical measurement. All photocurrent results shown in this study are the most representative results obtained from at least three measurements from three different samples for each sample type.

Results and Discussion

Bare Cu_2O photocathode The Cu_2O electrodes used in this study were prepared by electrodeposition.[3,15] It is composed of Cu_2O cubes that expose only the {100} facets (**Figure 1a-b**). As they grew with the {111} planes parallel to the substrate (equivalent to growing with the <111> direction, the body-diagonal of a cube, perpendicular to the substrate), each cube is shown as a trigonal pyramid (i.e., the truncated corner of a cube) (**Figure 1b**). As all Cu_2O crystals in the electrode have uniform orientations, the X-ray diffraction (XRD) pattern of the Cu_2O electrode obtained with the theta-two theta mode shows only the (111) peak. (This mode can record only the reflection peaks generated from the sets of planes parallel to the substrate.) (**Figure 1c**).

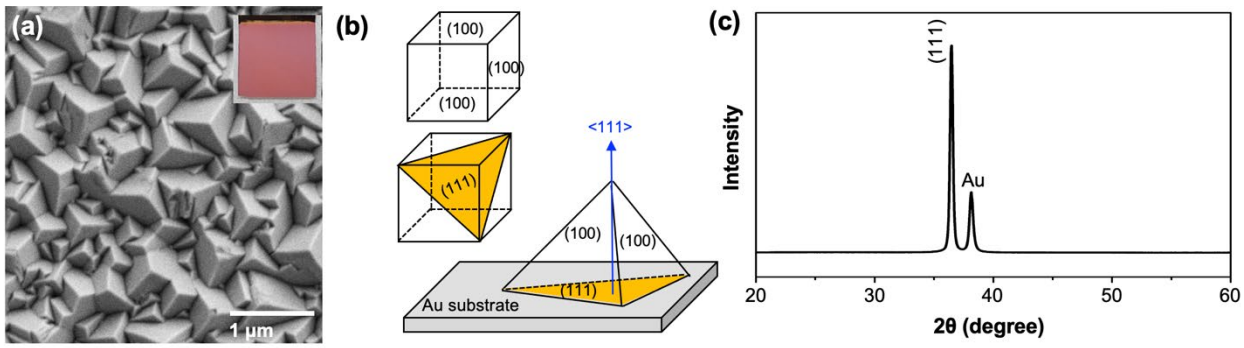

Figure 1. (a) SEM image and photograph of a Cu_2O electrode, (b) schemes explaining the exposed facets and orientation of Cu_2O cubes on the Au substrate, and (c) XRD pattern of a Cu_2O electrode.

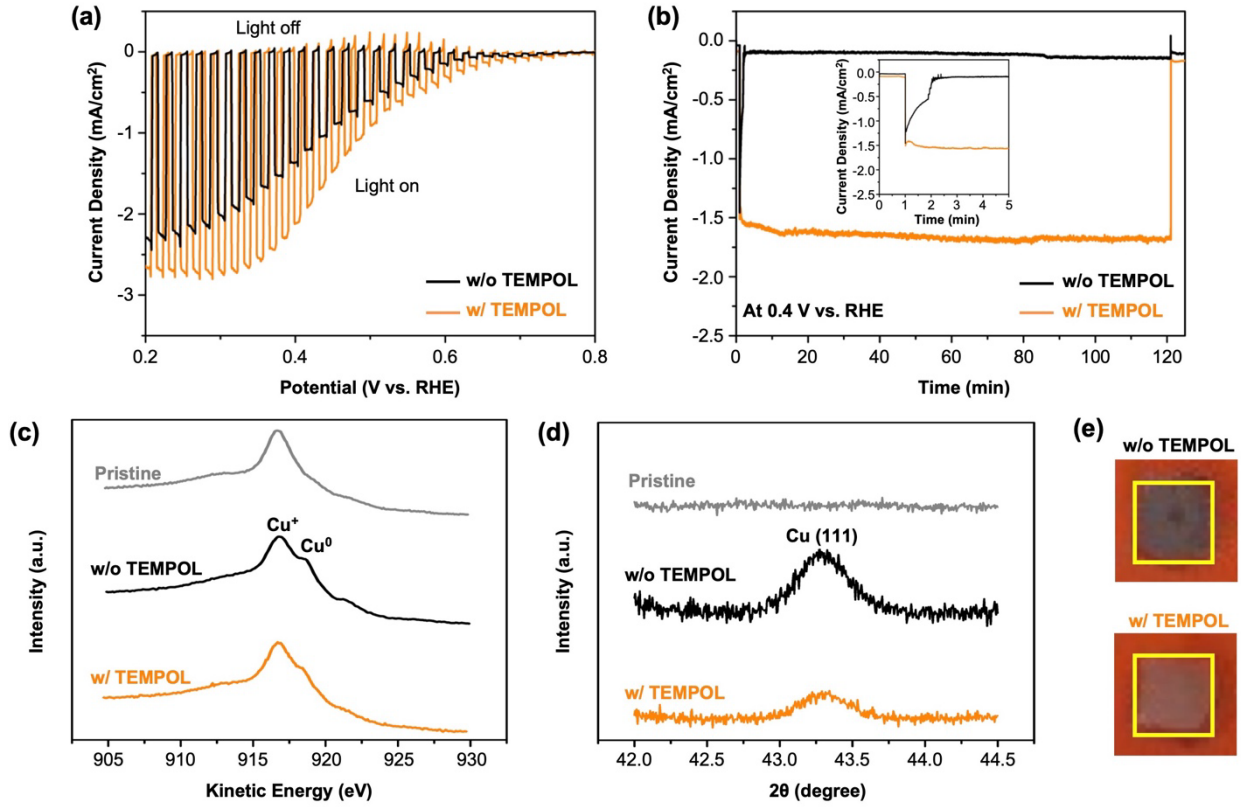

Figure 2. (a) J-V plots (10 mV/s) with chopped light and (b) J-t plots (at 0.4 V vs. RHE) of Cu_2O measured with (orange) and without (black) TEMPOL in a borate buffer (pH 10.6) under AM 1.5G illumination. The inset in (b) is an enlarged plot for the initial 5 min. (c) Cu LMM XPS spectra and (d) XRD patterns of Cu_2O (showing only the region for the most intense Cu (111) peak) after J-t measurement with (orange) and without (black) TEMPOL. (e) Photographs of a Cu_2O electrode after J-t measurement with (bottom) and without (top) TEMPOL. The illuminated region is indicated with a yellow box and has been enlarged for clarity (the actual illuminated area: 0.02 cm^2).

The photocurrent density vs. potential (J-V) and photocurrent density vs. time (J-t) plots obtained with the Cu_2O electrode with no electron scavenger are shown in **Figure 2a-b (black line)** where the Cu_2O electrode is used as a photocathode under AM 1.5G illumination in a borate solution (pH 10.6). The photocurrent density in the J-V plot is considerable (> 2 mA/cm^2 at 0.2 V vs. RHE), but the J-t plot shows that this photocurrent density decreases to almost 0 mA/cm^2 within a few minutes. This means that the photocurrent density shown in the J-V plot is not due to water reduction but is mainly associated with cathodic photocorrosion of Cu_2O; the recombination sites generated by photocorrosion of Cu_2O increase electron-hole recombination and eventually stop photocurrent generation. When the Cu_2O photocathode was analyzed by Cu LMM X-ray

photoelectron spectroscopy (XPS) and XRD after the J-t measurement, Cu metal formed by the cathodic photocorrosion of Cu_2O was detected (**Figure 2c-d**). Furthermore, the Cu_2O electrode was notably darkened after the J-t measurement (**Figure 2e, top**), which is a visible indication that cathodic photocorrosion occurred.

TEMPOL as an electron acceptor In this study, we used 4-hydroxy-2,2,6,6-tetramethylpiperidine-1-oxyl (TEMPOL) as an electron scavenger (**Figure 3**) to investigate the photoelectrochemical properties of Cu_2O photoelectrodes. While TEMPOL is widely known for its fast *oxidation* kinetics to its oxoammonium ion ($TEMPOL^+$),[18,19] we found that its reduction rate to its hydroxyl amine form (TEMPOL-H) is also sufficiently fast in slightly basic media (pH 10-11) and it can consume almost all of the surface reaching electrons in the Cu_2O photocathode before they are used for cathodic photocorrosion, thus kinetically suppressing cathodic photocorrosion of Cu_2O. This was proven by the J-V and J-t plots of Cu_2O obtained for TEMPOL reduction (**Figure 2a-b, orange line)**. The photocurrent density in the J-V plot obtained with TEMPOL is higher than that obtained without TEMPOL, indicating electron-hole recombination is reduced with the use of TEMPOL. More importantly, the initial photocurrent density in the J-t plot is sustained over two hours, meaning the majority of the photocurrent density shown in the J-V and J-t plots is not from cathodic photocorrosion but from TEMPOL reduction with the contribution from photocorrosion considerably diminished. To the best of our knowledge, this is the first time that a stable photocurrent was obtained during the J-t measurement of a bare Cu_2O photocathode over 2 hours, which indicates that TEMPOL is an effective electron scavenger for studying Cu_2O photocathodes.

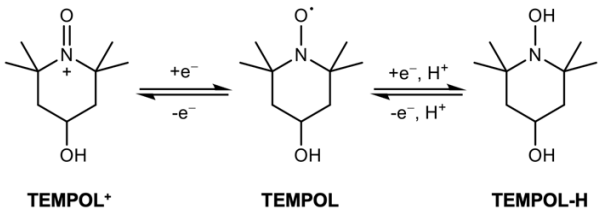

Figure 3. Redox reactions of TEMPOL; TEMPOL can be oxidized to $TEMPOL^+$ and reduced to TEMPOL-H.

The XPS and XRD analysis of the Cu_2O photocathodes after the J-t measurements with TEMPOL still detected the formation of Cu, meaning that the use of TEMPOL did not completely prevent photocorrosion (**Figure 2c-d**). However, although the total charge passed during the J-t measurement with TEMPOL was ~14 times greater than that without TEMPOL, the amount of Cu formed with TEMPOL during the J-t measurement is significantly less (less than ~50% judging from the Cu peaks in the XRD patterns) than that of the Cu formed without TEMPOL. This means that the fraction of photocurrent associated with photocorrosion during the 2 hours of J-t measurement with TEMPOL should be approximately less than 5%. The significant suppression of photocorrosion enabled by the use of TEMPOL is also visually evident; the surface darkening of the Cu_2O photocathode after generating a photocurrent density of ~1.5 mA/cm^2 with TEMPOL for 2 hours is much less severe than that after the J-t measurement without TEMPOL with a negligible amount of photocurrent generation (**Figure 2e**). This result is exciting as it confirms that the photocurrent density in the J-V plot for TEMPOL reduction can be directly related to the number of surface-reaching electrons available for interfacial charge transfer reactions.

ZnO and TiO_2 as an electron-extraction layer Next, we electrodeposited ZnO and TiO_2 layers on the Cu_2O electrode to examine their ability to extract electrons from the Cu_2O photocathode. A ZnO layer was electrodeposited using a deposition method that is known to form a highly transparent and crystalline ZnO layer,[17] and the detailed characterization and properties of this ZnO can be found in the previous study.[17] The SEM image and photograph of the Cu_2O/ZnO electrode (**Figure 4a)** show that ZnO on Cu_2O formed a transparent layer composed of round particles. As the ZnO layer changes the way the light reflects on the Cu_2O electrode surface, the color of Cu_2O in Cu_2O/ZnO looks brighter than that of the bare Cu_2O electrode (**Figure 1a**). The side-view SEM image of the Cu_2O/ZnO electrode shows that the thickness of the ZnO layer is approximately ~100 nm (**Figure S2**). This is an optimized thickness, meaning that increasing or decreasing the thickness of the ZnO layer results in a decrease in photocurrent generation by Cu_2O/ZnO photocathodes (**Figure S3**).

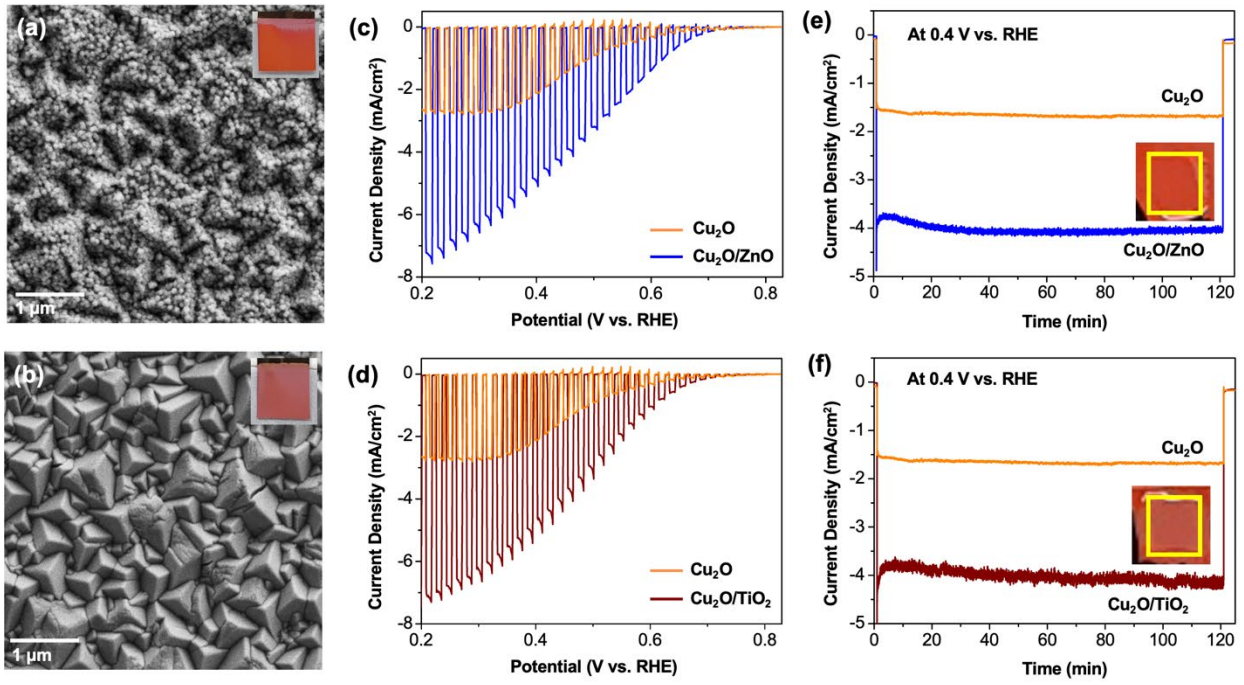

Figure 4. SEM and photographic images of (a) Cu_2O/ZnO and (b) Cu_2O/TiO_2. (c,d) J-V plots (10 mV/s) and (e,f) J-t plots (at 0.4 V vs. RHE) of Cu_2O/ZnO (top) and Cu_2O/TiO_2 (bottom) for TEMPOL reduction in a borate buffer (pH 10.6) under AM 1.5G illumination. The corresponding plots of pristine Cu_2O are also shown for comparison. The photographs shown in (e,f) are taken after the J-t measurement. The illuminated (inside the yellow box) and unilluminated regions look comparable for both Cu_2O/ZnO and Cu_2O/TiO_2 electrodes.

The TiO_2 layer was also electrodeposited using a previously reported method.[11] Unlike ZnO that is deposited as a crystalline phase, TiO_2 is deposited as a hydrated phase (TiO_xH_y) that needs to undergo a dehydration step to form TiO_2.[11] Thus, we annealed the as-prepared Cu_2O/TiO_2 electrodes at 200℃ for 2 h. The annealing was achieved in a tube furnace while flowing N_2 gas in order to not oxidize Cu_2O to CuO. After the annealing process, the Cu_2O/TiO_2 electrode was analyzed by XPS to confirm that no CuO was formed (**Figure S4**). The presence of the TiO_2 layer is not noticeable by SEM images or photographs of the Cu_2O/TiO_2 electrode because TiO_2 forms a conformal layer that is extremely thin. The transmission electron microscopy (TEM) image shows that it is ~5 nm thick (**Figure 5a**).

The J-V plot of Cu_2O/ZnO for TEMPOL reduction shows a considerable enhancement in photocurrent density, indicating that the electrodeposited ZnO layer can serve as an excellent electron extraction layer (**Figure 4c**). For example, the photocurrent density at 0.2 V vs. RHE increased from 2.7 mA/cm^2 to 7.2 mA/cm^2. The J-t plot shows that the photocurrent enhanced by

ZnO can be sustained over 2 h (**Figure 4e**). As ZnO can rapidly extract electrons reaching the Cu_2O surface, the chance of the surface reaching electrons being used for photocorrosion should decrease. Indeed, the XRD pattern after the J-t measurement shows no detectable Cu peaks (**Figure 6**). (Cu LMM XPS spectra can no longer be used to detect Cu because XPS is a surface technique and the surface of Cu_2O is covered by ZnO.) Also, the photograph of the Cu_2O/ZnO electrode shows no visible difference between the illuminated and unilluminated regions after the J-t measurement. This demonstrates that the ability of ZnO to extract surface-reaching electrons from Cu_2O is directly related to its ability to suppress corrosion in Cu_2O when the extracted electrons can be rapidly consumed for TEMPOL reduction. We note that in the previous studies where ALD-deposited ZnO was used as a buffer layer on Cu_2O, it was reported that Al doping in the ZnO layer was needed.[1,5-7] However, judging from the fact that our electrodeposited ZnO layer can efficiently extract electrons from Cu_2O without requiring Al doping, it appears that this requirement is only for ALD-deposited ZnO that is not sufficiently conductive. We also note that while ZnO can serve as an effective electron extraction layer, it is amphiphilic and it is stable only in slightly basic media, meaning it requires a protection layer when used in other pH conditions. (This study used the pH where ZnO is chemically stable as the goal is to compare the electron extraction abilities of ZnO and TiO_2 not affected by other factors.)

The J-V plot of the Cu_2O/TiO_2 photocathode also shows a considerable enhancement in photocurrent density comparable to that observed with the Cu_2O/ZnO photocathode (**Figure 4d**), indicating that TiO_2 can also efficiently extract electrons from Cu_2O. This result is surprising as previous studies on Cu_2O photocathodes reported that TiO_2 cannot efficiently extract electrons from Cu_2O.[1,5-8] The J-t plot of Cu_2O/TiO_2 also shows stable photocurrent generation (**Figure 4f**), confirming that the photocurrent shown in the J-V and J-t plots is primarily due to TEMPOL reduction. As in the case of Cu_2O/ZnO, the rapid extraction of electrons from the Cu_2O by the TiO_2 layer reduced the degree of photocorrosion in the Cu_2O layer as confirmed by the photograph of the Cu_2O/TiO_2 photocathode after the J-t measurement. Also, the XRD pattern of the Cu_2O/TiO_2 photocathode after the J-t measurement showed the Cu (111) peak that is barely noticeable (**Figure 6**).

Comparison of TiO_2 Layers Formed by Electrodeposition and ALD As the electrodeposited TiO_2 layer on Cu_2O behaves quite differently from ALD-deposited TiO_2 layers on Cu_2O reported

in previous studies,[1,5-8] we also prepared a Cu_2O/TiO_2 (ALD) photocathode by depositing a TiO_2 layer by ALD. This way we can compare the performances of Cu_2O/TiO_2 (ALD) with our Cu_2O/TiO_2 side-by-side under the same measurement conditions. The thickness of the ALD-deposited TiO_2 layer was adjusted to be the same (~5 nm) as that of the electrodeposited TiO_2 layer (**Figure 5a-b**).

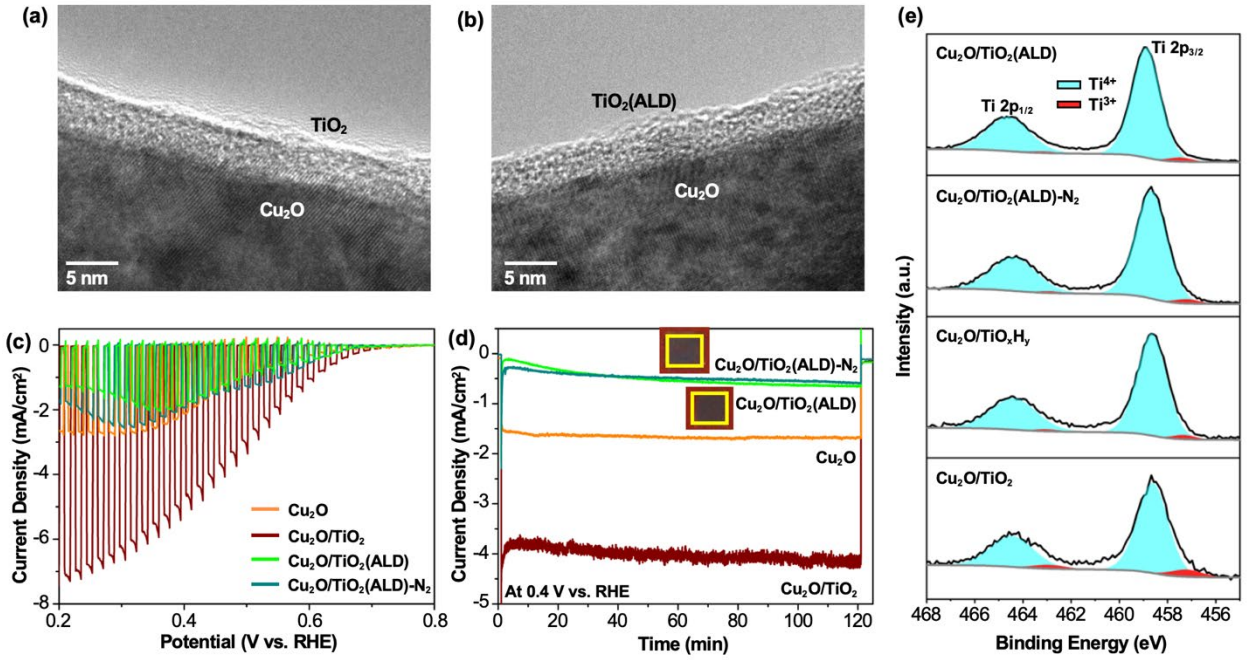

Figure 5. TEM images of (a) Cu_2O/TiO_2 and (b) Cu_2O/TiO_2(ALD), (c) J-V plots (10 mV/s) and (d) J-t plots (at 0.4 V vs. RHE) of Cu_2O/TiO_2(ALD) for TEMPOL reduction in a borate buffer (pH 10.6) under AM 1.5G illumination compared with those of Cu_2O, Cu_2O/TiO_2, and Cu_2O/TiO_2(ALD)-N_2. The insets in (d) are photographs of Cu_2O/TiO_2(ALD) and Cu_2O/TiO_2(ALD)-N_2 photoelectrodes after the J-t measurement. (e) Ti 2p XPS spectra of the TiO_2 layer in Cu_2O/TiO_xH_y, Cu_2O/TiO_2, and Cu_2O/TiO_2(ALD) before and after annealing with N_2, where the contributions from Ti^{3+} and Ti^{4+} are deconvoluted.

The J-V and J-t plots of the Cu_2O/TiO_2(ALD) are shown in **Figure 5c-d** compared to those of Cu_2O and Cu_2O/TiO_2. The photocurrent density of Cu_2O/TiO_2(ALD) in the J-V plot is no higher or even less than that of Cu_2O. The photocurrent density obtained with the J-t measurement at 0.4 V vs. RHE is also significantly less than that of Cu_2O. This means that TiO_2(ALD) does not serve as a good electron extraction layer and its presence causes more cathodic photocorrosion and electron-hole recombination. (The photocurrent decrease observed below 0.36 V vs. RHE in the

J-V plot also appears to be due to more severe photocorrosion occurring during the J-V measurement.) The post J-t analysis of the Cu_2O/TiO_2(ALD) photoelectrode shows more severe darkening of the electrode surface and formation of more Cu in the XRD pattern compared to that of the bare Cu_2O electrode (**Figure 6**). This result shows that although TiO_2 is chemically and electrochemically inert, it cannot serve as a good protection layer for photocorrosion if it cannot efficiently extract photogenerated electrons from the Cu_2O layer. This result agrees well with the previous results obtained with ALD-deposited TiO_2 protection layers.[1]

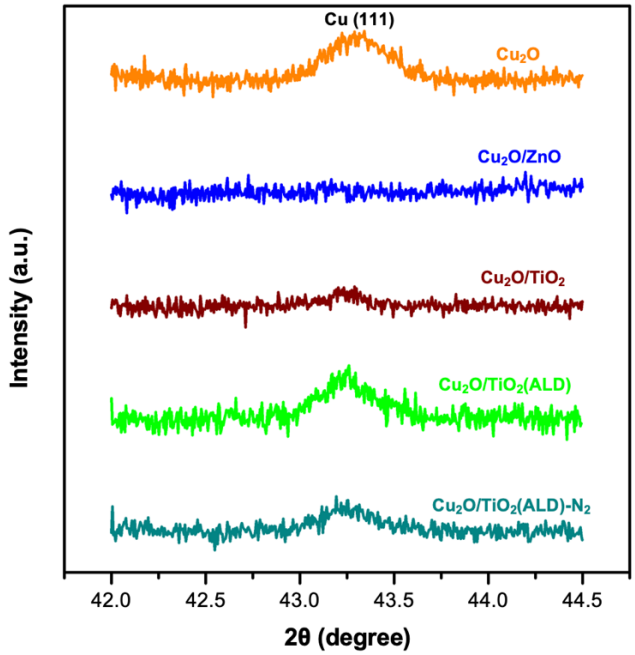

Figure 6. XRD patterns of Cu_2O, Cu_2O/ZnO, Cu_2O/TiO_2, Cu_2O/TiO_2(ALD), and Cu_2O/TiO_2(ALD)-N_2 after the J-t measurement for TEMPOL reduction.

The comparison of electrodeposited and ALD-deposited TiO_2 layers on Cu_2O is intriguing as it demonstrates that the performance of the TiO_2 as an electron extraction layer is strikingly affected by the deposition method. We recognized that the electrodeposited TiO_2 layer underwent a post-deposition annealing treatment in an N_2 environment to dehydrate the as-deposited TiO_2 layer. Thus, in case the observed difference is due to this annealing process, we also annealed the Cu_2O/TiO_2(ALD) photocathode under the same conditions. However, no noticeable difference was observed in the J-V and J-t plots after this treatment (**Figure 5c-d**, labeled as Cu_2O/TiO_2(ALD)-N_2).

We obtained and compared Ti 2p XPS spectra of the TiO_2 layer in Cu_2O/TiO_2 and Cu_2O/TiO_2(ALD) photoelectrodes to examine if there is any apparent difference between the two TiO_2 layers that may be related to the observed performance differences (**Figure 5e**). The result shows that the Ti^{3+} contents in these two TiO_2 layers are different. The Ti^{3+} content in the ALD-deposited TiO_2 layer is ~3% Ti^{3+} and it does not increase by annealing at 200 °C in N_2, meaning that annealing at 200 °C in N_2 is insufficient to reduce Ti^{4+} to Ti^{3+} in the ALD-deposited TiO_2 layer. In contrast, while the Ti^{3+} content in the as-deposited, hydrated TiO_xH_y layer prepared by electrodeposition is also ~3%, it increases to ~7% after annealing at 200 °C in N_2. This is because the structure of the electrodeposited, hydrated TiO_xH_y layer is not as rigid as the ALD-deposited TiO_2 layer. When TiO_xH_y undergoes structural and compositional changes to form TiO_2 via dehydration at 200 °C in N_2, the given annealing condition appears to be sufficient to create O vacancies and corresponding Ti^{3+} (to balance the charge) in the TiO_2 layer. The higher Ti^{3+} and associated O vacancy contents in the electrodeposited TiO_2 layer can make the TiO_2 layer more conductive for electrons because O vacancies can serve as donors to increase the carrier density in TiO_2.[20] Also, the more n-type nature of the TiO_2 layer may result in more favorable band alignments with the Cu_2O layer to make electron injection from the CB of Cu_2O to the CB of TiO_2 energetically more favorable. Thus, the higher Ti^{3+} and O vacancy content of the electrodeposited TiO_2 layer is likely one of the factors that make the electrodeposited TiO_2 layer a superior electron-extraction layer to the ALD-deposited TiO_2 layer.

As the two deposition methods are quite different in terms of deposition conditions (solution vs. gas phase deposition), precursors for Ti, and wetness of the Cu_2O surface during deposition, we think it is also possible that the local structures of the outermost Cu and the first layer of Ti on Cu_2O can be quite different at the Cu_2O/TiO_2 and Cu_2O/TiO_2(ALD) interfaces. This difference may be such that less interfacial recombination sites are formed at the Cu_2O/TiO_2 junction than at the Cu_2O/TiO_2(ALD) junction. We will continue to investigate various factors that can affect the ability of electron-extraction layers used in multilayer photoelectrodes.

The direct performance comparison of Cu_2O/TiO_2(electrodeposition) and Cu_2O/TiO_2(ALD) photocathodes made in this study for the first time revealed that even for the same TiO_2 material, the detailed features affected by deposition methods can considerably alter its ability to serve as an electron extraction layer on Cu_2O. This understanding, in turn, suggests that the performance of the TiO_2 layer as an electron-extraction layer on Cu_2O may improve if the conditions of any

deposition method can be modified to create an optimal content of Ti^{3+} in TiO_2. By better understanding the factors that affect electron transfer in multilayer photoelectrodes, it will be possible to rationally optimize the performance of multilayer photoelectrodes.

Conclusions

In summary, we demonstrated the use of TEMPOL as an effective electron scavenger to study photoelectrochemical properties of Cu_2O modified by buffer and protection layers. The reduction kinetics of TEMPOL are fast enough to consume the majority of surface-reaching electrons before these electrons are consumed by photocorrosion of Cu_2O. As a result, photocurrent obtained by TEMPOL could be primarily related to the number of surface-reaching electrons available for interfacial charge transfer reactions, while photocurrent obtained without TEMPOL is primarily associated with photocorrosion and is affected by the resulting electron-hole recombination. Therefore, any change in the photocurrent for TEMPOL reduction after a buffer or protection layer was added could be directly linked to the ability of these layers to enhance or decrease electron-hole recombination in the Cu_2O layer. Our results showed that both the electrodeposited ZnO and TiO_2 layers can serve as excellent electron extraction layers and can suppress photocorrosion in the Cu_2O layer. When a Cu_2O/TiO_2 photocathode was prepared with a TiO_2 layer with the same thickness deposited by ALD, the performance of the resulting Cu_2O/TiO_2(ALD) photocathode was not any better than a bare Cu_2O photocathode, which agrees with the previous studies. This result suggests that the detailed features of the TiO_2 layer that can be altered by deposition methods, such as the level of intrinsic defects and conductivity, have a striking impact on the interfacial charge transfer at the Cu_2O/TiO_2 junction. The new method and understanding provided in this study will help to facilitate the selection, testing, and optimization of buffer and protection layers.

ASSOCIATED CONTENT

Supporting Information

The Supporting Information is available free of charge on the ACS Publication website:

A side-view SEM image of a Cu_2O/ZnO photocathode and J-V plots of Cu_2O/ZnO photocathodes used to optimize the thickness of the ZnO layer.

Competing interests

The authors declare no competing interests.

AUTHOR INFORMATION

Corresponding Author

*Email: kschoi@chem.wisc.edu

Acknowledgments

This work was support by the Division of Chemical Sciences, Geosciences, and Biosciences, Office of Basic Energy Sciences of the U.S. Department of Energy through Grant DE-SC0008707. The TiO_2 (ALD) films were deposited using the Materials Synthesis and Characterization facilities of the Center for Functional Nanomaterials, which is a U.S. DOE Office of Science Facility, at Brookhaven National Laboratory under Contract No. DE-SC0012704.

References

(1) Paracchino, A.; Laporte, V.; Sivula, K.; Grätzel, M.; Thimsen, E. Highly Active Oxide Photocathode for Photoelectrochemical Water Reduction. *Nat. Mater.* **2011**, *10*, 456–461.

(2) Liu, G.; Zheng, F.; Li, J.; Zeng, G.; Ye, Y.; Larson, D. M.; Yano, J.; Crumlin, E. J.; Ager, J. W.; Wang, L.; Toma, F. M. Investigation and Mitigation of Degradation Mechanisms in Cu_2O Photoelectrodes for CO_2 Reduction to Ethylene. *Nat. Energy* **2021**, *6*, 1124–1132.

(3) Jang, Y. J.; Lindberg, A. E.; Lumley, M. A.; Choi, K.-S. Photoelectrochemical Nitrogen Reduction to Ammonia on Cupric and Cuprous Oxide Photocathodes. *ACS Energy Lett.* **2020**, *5*, 1834–1839.

(4) Lumley, M. A.; Radmilovic, A.; Jang, Y. J.; Lindberg, A. E.; Choi, K.-S. Perspectives on the Development of Oxide-Based Photocathodes for Solar Fuel Production. *J. Am. Chem. Soc.* **2019**, *141*, 18358−18369.

(5) Luo, J.; Steier, L.; Son, M.-K.; Schreier, M.; Mayer, M. T.; Grätzel, M. Cu_2O Nanowire Photocathodes for Efficient and Durable Solar Water Splitting. *Nano Lett.* **2016**, *16*, 1848–1857.

(6) Morales-Guio, C. G.; Tilley, S. D.; Vrubel, H.; Grätzel, M.; Hu, X. Hydrogen Evolution from a Copper(I) Oxide Photocathode Coated with an Amorphous Molybdenum Sulphide Catalyst. *Nat. Commun.* **2014**, *5*, 3059.

(7) Tilley, S. D.; Schreier, M.; Azevedo, J.; Stefik, M.; Grätzel, M. Ruthenium Oxide Hydrogen Evolution Catalysis on Composite Cuprous Oxide Water-Splitting Photocathodes. *Adv. Funct. Mater.* **2014**, *24*, 303–311.

(8) Pan, L.; Kim, J. H.; Mayer, M. T.; Son, M.-K.; Ummadisingu, A.; Lee, J. S.; Hagfeldt, A.; Luo, J.; Grätzel, M. Boosting the Performance of Cu_2O Photocathodes for Unassisted Solar Water Splitting Devices. *Nat. Catal.* **2018**, *1*, 412−420.

(9) Schmets, J.; Muylder, J. V.; Pourbaix, M. Titanium. In *Atlas of Electrochemical Equilibria in Aqueous Solutions*, 2nd ed.; NACE: Houston, TX, 1974; pp 213–222.

(10) Hu, S.; Shaner, M. R.; Beardslee, J. A.; Lichterman, M.; Brunschwig, B. S.; Lewis, N. S. Amorphous TiO_2 Coatings Stabilize Si, GaAs, and GaP Photoanodes for Efficient Water Oxidation. *Science*, **2014**, *344*, 1005–1009.

(11) Lee, D.; Kvit, A.; Choi, K.-S. Enabling Solar Water Oxidation by $BiVO_4$ Photoanodes in Basic Media. *Chem. Mater.* **2018**, *30*, 4704–4712.

(12) Zhao, J.; Minegishi, T.; Zhang, L.; Zhong, M.; Gunawan; Nakabayashi, M.; Ma, G.; Hisatomi, T.; Katayama, M.; Ikeda, S.; Shibata, N.; Yamada, T.; Domen, K. Enhancement of Solar Hydrogen Evolution from Water by Surface Modification with CdS and TiO_2 on Porous $CuInS_2$ Photocathodes Prepared by an Electrodeposition–Sulfurization Method. *Angew. Chem. Int. Ed.* **2014**, *53*, 11808–11812.

(13) Yang, W.; Kim, J. H.; Hutter, O. S.; Phillips, L. J.; Tan, J.; Park, J.; Lee, H.; Major, J. D.; Lee, J. S.; Moon, J. Benchmark Performance of Low-Cost Sb_2Se_3 Photocathodes for Unassisted Solar Overall Water Splitting. *Nat. Commun.* **2020**, *11*, 861.

(14) Yun, J.; Tan, J.; Jung, Y.-K.; Yang, W.; Lee, H.; Ma, S.; Park, Y. S.; Lee, C. U.; Niu, W.; Lee, J.; Kim, K.; Tilley, S. D.; Walsh, A.; Moon, J. Interfacial Dipole Layer Enables High-Performance Heterojunctions for Photoelectrochemical Water Splitting. *ACS Energy Lett.* **2022**, *7*, 1392–1402.

(15) McShane, C. M.; Siripala, W. P.; Choi, K.-S. Effect on Junction Morphology on the Performance of Polycrystalline Cu_2O Homojunction Solar Cells. *J. Phys. Chem. Lett.* **2010**,

1, 2666–2670.
(16) McDonald, K. J.; Choi, K.-S. A New Electrochemical Synthesis Route for a BiOI Electrode and Its Conversion to a Highly Efficient Porous $BiVO_4$ Photoanode for Solar Water Oxidation. *Energy Environ. Sci.* **2012**, *5*, 8553–8557.
(17) Kang, D.; Lee, D.; Choi, K.-S. Electrochemical Synthesis of Highly Oriented, Transparent, and Pinhole-Free ZnO and Al-Doped ZnO Films and Their Use in Heterojunction Solar Cells. *Langmuir* **2016**, *32*, 10459–10466.
(18) Liu, T.; Wei, X.; Nie, Z.; Sprenkle, V.; Wang, W. A Total Organic Aqueous Redox Flow Battery Employing a Low Cost and Sustainable Methyl Viologen Anolyte and 4-HO-TEMPO Catholyte. *Adv. Energy Mater.* **2016**, *6*, 1501449.
(19) Nam, D.-H.; Choi, K.-S. Tandem Desalination/Salination Strategies Enabling the Use of Redox Couples for Efficient and Sustainable Electrochemical Desalination. *ACS Appl. Mater. Interfaces* **2019**, *11*, 38641–38647.
(20) Mao, C.; Zuo, F.; Hou, Y.; Bu, X.; Feng, P. In Situ Preparation of a Ti^{3+} Self-Doped TiO_2 Film with Enhanced Activity as Photoanode by N_2H_4 Reduction. *Angew. Chem. Int. Ed.* **2014**, *53*, 10485–10489.

TOC Graphic

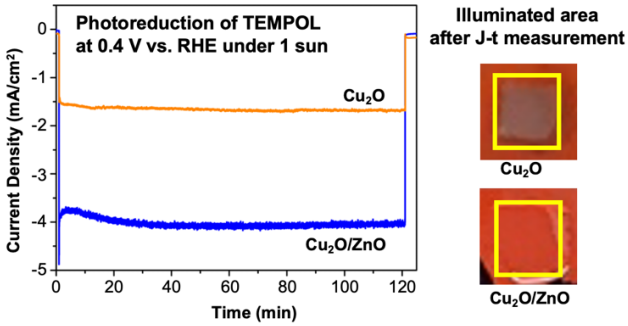
Photoreduction of TEMPOL
at 0.4 V vs. RHE under 1 sun
Cu2O
Cu2O/ZnO
Current Density (mA/cm²)
Time (min)
0
-1
-2
-3
-4
-5
0
20
40
60
80
100
120
Illuminated area
after J-t measurement
Cu2O
Cu2O/ZnO